2025 IEEE World Haptics Conference (WHC)
Suwon Convention Center, Suwon, Korea
July 8 ~ 11, 2025

OptiStrain: A Vision- and Microfluidics-based Tactile Sensor with High Spatial and Temporal Resolution

Evan Harber[1], Colin P. Johnson[1], Ahuvah Liebman[1], Andreas Psychoyos[1], Mumbi Whidby[1], Sung-Min Kang[2], Jimmy Penaloza[1], Andrew T. Bender[3], Jonathan D. Posner[3], and Veronica J. Santos[1]

I. Introduction

Human touch relies on a combination of high spatial resolution (25–100 points/cm^2) and high temporal resolution (<1000 Hz) to distinguish textures and enable effective grasping and manipulation of various objects [1], [2]. Previous tactile sensors have captured some, but not all, aspects of human touch. For example, optical tactile sensors such as the GelSight [3], TacTip [4] and Soft-bubble [5] use cameras to visually track the deformation of a contact surface with high spatial resolution, but are typically limited to sampling rates of 30 or 60 fps. Other sensors, such as the BioTac [6] and sensors based on magnetic principles [7] and liquid metal strain gauges [8], have significantly higher temporal resolution. As a result, such sensors can detect rapid changes in fluid pressure, magnetic fields, and electrical resistance, respectively, but have lower spatial resolution when compared to camera-based sensors.

In this work, we introduce a multimodal tactile sensor called "OptiStrain," which combines high spatial and temporal resolution capabilities. High spatial resolution is achieved through vision-based sensing (as in Yuan *et. al.* [3]) while high temporal resolution is achieved through a liquid metal strain gauge embedded in the sensor's elastomeric fingerpad (as in Yin *et. al.* [8]). This approach enables the sensor to capture detailed, local spatial geometry as well as small magnitude, rapidly changing electrical signals. We demonstrate that this framework not only maps force distributions across a surface but also detects subtle deformations with enhanced precision.

To showcase these benefits, we conducted a qualitative analysis to demonstrate the complementary benefits of each sensor modality. We captured contact area via image data. We measured small strains via a liquid metal strain gauge. Furthermore, we demonstrated how combining the data streams can be used to train a network to estimate normal contact force. Incorporating both sensing modalities decreased force estimation error by 12% and 14% as compared to image-only inputs and strain gauge-only inputs, respectively. **To the best of our knowledge, the OptiStrain is the first multimodal tactile sensor that integrates vision-based and microfluidics-based sensing mechanisms.**

Supported in part by Office of Naval Research Award #N00014-23-1-2842 and Univ. of California Office of the President, Multicampus Research Prog. and Init. Award #M21PR3492. Any opinions, findings, and conclusions or recommendations expressed in this material are those of the authors and do not necessarily reflect the views of the funding agencies.

[1]Dept. of Mechanical and Aerospace Engin., University of California, Los Angeles, CA 90095. e-mail: eharber@ucla.edu
[2]Dept. of Elec. & Comp. Engin., Univ. of Washington, Seattle, WA 98195
[3]Dept. of Mechanical Engin., Univ. of Washington, Seattle, WA 98195.

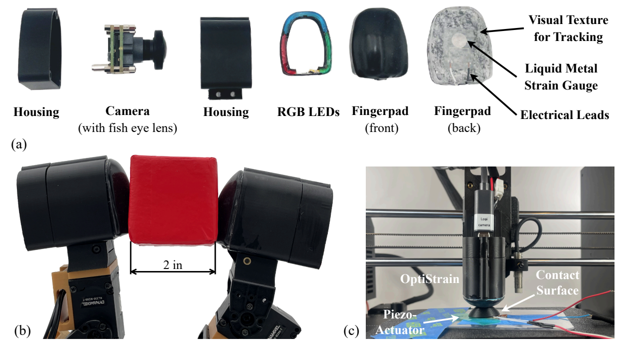

Fig. 1: (a) Overview of the main components of the OptiStrain tactile sensor. (b) Two OptiStrain sensor fingertips grasping a block. (c) Experimental setup.

II. Experimental Procedure

A. Sensor Design

The OptiStrain multimodal tactile sensor is comprised of two primary sets of components for measuring spatial and temporal tactile information (Fig. 1a):

The **vision-based component for high spatial resolution** consists of a camera (TechNexion UVCI-AR0234-C-S128-IR) and fisheye lens (EDATEC ED-LENS-M12-280167-08) positioned to face a deformable, optically clear, elastomeric fingerpad (Smooth-On Solaris™) mounted to a rigid, 3D-printed housing. The fingerpad is bonded to an acrylic layer (Smooth-On SIL-poxy™) that is glued to the rest of the housing. To facilitate optical flow-based tracking, we apply a finish to the outer surface of the elastomeric fingerpad using random speckles of paint (Smooth-On Silc Pig™), which adds a visual texture, similar to the Soft-bubble sensor [5].

The **liquid metal strain gauge-based component for high temporal resolution** is fabricated by spin-coating an elastomer (Smooth-On Dragon Skin™ 30) over a photolithographically spiral-patterned mold and a flat mold. After curing, holes are punched at both ends of the spiral channel using a syringe and the two layers are bonded together via liquid fusion. Eutectic gallium indium is vacuum-filled into the microfluidic channel, and copper wires are attached as terminals. The liquid metal strain gauge is then embedded in the optically clear elastomeric fingerpad by curing a base layer, placing the liquid metal strain gauge, and pouring the remaining elastomer.

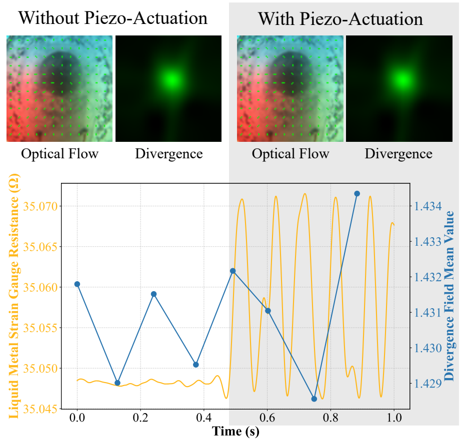

Fig. 2: Representative OptiStrain data are shown for two different strain conditions (Fig 1c). (Top) The contact region for the hemispherical object is visible, but the effects of piezo-actuation are not observable in the optical flow fields or divergence of the flow fields. (Bottom) The liquid metal strain gauge is highly sensitive to small strains imposed by piezo-actuation.

B. Data Collection

A modified 3D printer (Prusa i3 MK3S) was used to collect preliminary tactile sensor data by systematically pressing the OptiStrain sensor against a 3D-printed, hemispherical object (Fig. 1c). A thin piezoelectric actuator (APC PZT - Type 855) or a 6-DOF load cell (ATI Nano25) was placed beneath the hemispherical object to facilitate our qualitative study or force calibration, respectively. To measure changes in voltage across the liquid metal strain gauge, we built a voltage divider with a 47Ω resistor in series with the strain gauge, powered by an external 5V power supply. A data acquisition system recorded the strain gauge and force-torque sensor data at up to 100 kHz to ensure high temporal-resolution data acquisition.

III. Results and Discussion

Qualitative Analysis. To demonstrate the individual contributions of each sensing modality, we collected OptiStrain data during a constant strain with and without high frequency piezo-actuation; representative data are shown in Fig. 2. Farneback's optical flow algorithm [5] was used to create a flow field and estimate contact pressure via flow field divergence. At $t \approx 0.5$s, we drove the piezo-actuator with a 10 Hz, 300V signal—corresponding to approximately $\pm$ 0.12 µm strain. The optical flow algorithm captured the shape of the contact region. However, there were no observable effects of piezo-actuation in the vision-based data. Importantly, the liquid metal strain gauge was highly sensitive to the small strains imposed by the piezo-actuator. Strain gauge data are shown after applying a forward and backward pass of a second-order Butterworth filter with a 30 Hz cut-off freq.

Force Calibration. To quantify the benefit of combining data streams, we generated training and testing datasets using the 3D printer setup (Fig. 1c). The OptiStrain fingerpad was pressed into the force-torque sensor at various normal contact forces (0-12N), force loading rates, and contact angles.

We trained LSTM networks to estimate the normal force measured by the force-torque sensor. Models were trained using different feature vectors: (i) only image features extracted

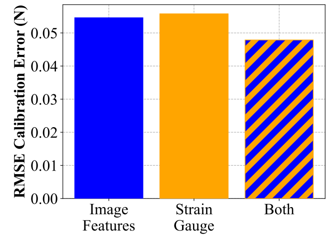

Fig. 3: Force calibration models were trained using image features, strain gauge data, and both types of data simultaneously. The model based on pooled data outperformed the models based on only one data type.

by the VGG-16 model [9], (ii) only strain gauge data, and (iii) pooled image features and strain gauge data. The LSTM received five sequential feature vectors captured 33ms apart. All models were trained for 1000 epochs with a learning rate of 1e-6 using the Adam optimizer.

As shown in Fig. 3, all models achieved sub-Newton accuracy across the 12N force range. The multimodal model outperformed the unimodal models – estimation errors were reduced by 12% and 14% as compared to image-only inputs and strain gauge-only inputs, respectively.

IV. Conclusion and Future Work

In this work, we present OptiStrain, a multimodal tactile sensor that combines vision- and microfluidics-based sensing into a single elastomeric fingerpad. This unified design captures high-resolution spatial and temporal data simultaneously. First, we demonstrate the sensor's utility in a qualitative study and show how it measures contact area and micron-scale strain. Then, we quantify how merging the camera and strain gauge data streams improves the accuracy of normal force estimates.

In future work, we will use the OptiStrain sensor to develop tactile perception algorithms for local shape and texture classification, and leverage these perceptual insights to enhance contact-aware grasp and manipulation capabilities for robotic systems.

V. Acknowledgments

The authors thank Bryn Spilker, Cole Ten, and Dr. Dustin Tyler for contributing to the initial sensor concept, Cole Ten for assistance with the 3D printer and data acquisition, and Dr. Kotekar P. Mohanchandra and Dr. Gregory Carman for their assistance with the piezo-actuator.

References

[1] A. Vallbo et al., "Properties of cutaneous mechanoreceptors in the human hand related to touch sensation," *H. Neurobiol.*, pp. 3–14, 1984.
[2] S. Lederman et al., "Haptic perception: A tutorial," *Attention, Perception, & Psychophysics*, pp. 1439–1459, 2009.
[3] W. Yuan et al., "GelSight: High-resolution robot tactile sensors for estimating geometry and force," *Sensors*, 2017.
[4] B. Ward-Cherrier et al., "The tactip family: Soft optical tactile sensors with 3d-printed biomimetic morphologies," *So. Ro.*, pp. 216–227, 2018.
[5] A. Alspach et al., "Soft-bubble grippers for robust and perceptive manipulation," in *IROS*, 2020, pp. 9917–9924.
[6] N. Wettels et al., "Biomimetic tactile sensor array," *Adv. Robot.*, pp. 829–849, 2008.
[7] K. Dai et al., "Design of a biomimetic tactile sensor for material classification," in *ICRA*, 2022, pp. 10 774–10 780.
[8] J. Yin et al., "Measuring dynamic shear force and vibration with a bioinspired tactile sensor skin," *Sensors*, pp. 3544–3553, 2018.
[9] W. Yuan et al., "Shape-independent hardness estimation using deep learning and a gelsight tactile sensor," *CoRR*, 2017.